N87-21815

RAPID SOFT X-RAY FLUCTUATIONS IN SOLAR FLARES OBSERVED WITH THE X-RAY POLYCHROMATOR

D. M. Zarro and J. L. R. Saba

Applied Research Corporation
Landover, MD

K. T. Strong

Lockheed Palo Alto Research Laboratories
Palo Alto, CA

ABSTRACT

We have studied three flares observed by the Soft X-Ray Polychromator on the Solar Maximum Mission. Flare light curves from the Flat Crystal Spectrometer and Bent Crystal Spectrometer were examined for rapid signal variations. Each flare was characterized by an initial fast (<1 min) burst, observed by the Hard X-Ray Burst Spectrometer (HXRBS), followed by softer gradual X-ray emission lasting several minutes. From an autocorrelation function analysis, we have found evidence for quasi-periodic fluctuations with rise and decay times of 10 s in the Ca XIX and Fe XXV light curves. These variations were of small amplitude (<20%), often coincided with hard X-ray emissions, and were prominent during the onset of the gradual phase after the initial hard X-ray burst. We speculate that these fluctuations were caused by repeated energy injections in a coronal loop that had already been heated and filled with dense plasma associated with the initial hard X-ray burst.

1. INTRODUCTION

Soft X-ray emission from solar flares is usually characterized by timescales ranging from several minutes to many hours. However, this impression is based on observations by instruments of limited spatial, spectral, and temporal resolution and coverage. In this paper we use Solar Maximum Mission (SMM) observations to demonstrate the existence of soft X-ray fluctuations with faster timescales of seconds to minutes.

The X-Ray Polychromator (XRP) on board the SMM is composed of two soft X-ray instruments: the Bent Crystal Spectrometer (BCS) and the Flat Crystal Spectrometer (FCS) (Acton *et al.* 1980). These instruments are ideal for high time resolution studies since they have good temporal resolution (0.5-10 s for the BCS and 0.256 s for the FCS), high spectral resolution ($\lambda/\delta\lambda > 1000$), and well-collimated fields of view (6 arcmin FWHM for the BCS and 14 arcsec FWHM for the FCS). Among the various techniques for analysing time series data, the autocorrelation function (ACF) provides a direct method of extracting the mean timescale of rapid variations that are superimposed on a slowly varying background (Jenkins and Watts 1968). The following is a brief description of the technique and its application.

Given a sequence of N observations $Y(i)$, the ACF is calculated by the formula:

$$\mathrm{ACF}(u) = \sum_{i=1}^{N-u} [Y(i) - \langle Y \rangle][Y(i+u) - \langle Y \rangle],$$

where u is the lag time in units of the accumulation time and $< Y >$ is the data mean. For statistically significant variations in the data, the characteristic timescale is related to the $1/e$ width of the ACF (Jenkins and Watts, 1968). This relationship is demonstrated in the following simulation. We model a fluctuating data stream by a first order autoregressive series defined by the algorithm:

$$Y(i) = aY(i-1) + bZ + c,$$

where Z denotes a random noise variable and $\tau = -\ln(a)^{-1}$ is the characteristic fluctuation timescale. The constants b and c are chosen such that the mean and variance of the autoregressive series match those of the observations. For example, figure 1a shows an example of fluctuations with $\tau = 17.5$ s, generated with a poisson noise random number generator. Figure 1b illustrates the corresponding ACF with a superposed exponential fit based on the first ten points. The timescale implied by this function is approximately $\tau = 20$ s. The error in this value may be estimated via a simple iterative procedure whereby a new autoregressive series is generated based on the current τ. An autocorrelation function is then calculated and a new τ derived. This procedure is repeated to yield a set of timescales from which a corresponding mean and standard deviation can be assigned. Thus, in the above example, five iterations with different random number seeds gave $\tau = 19.5 \pm 4$ s. Note that the autocorrelation width is an approximate measure of the mean temporal width of spike-like enhancements occuring within the data train. Hence, for example, an autocorrelation width of less than 20 s would imply that the rise and decay times of significant fluctuations are typically faster than 10 s (i.e., $\tau_{rise} \approx \tau_{ACF}/2$). In the following section we apply this autocorrelation technique to X-ray light curves for three strong solar flares observed with SMM.

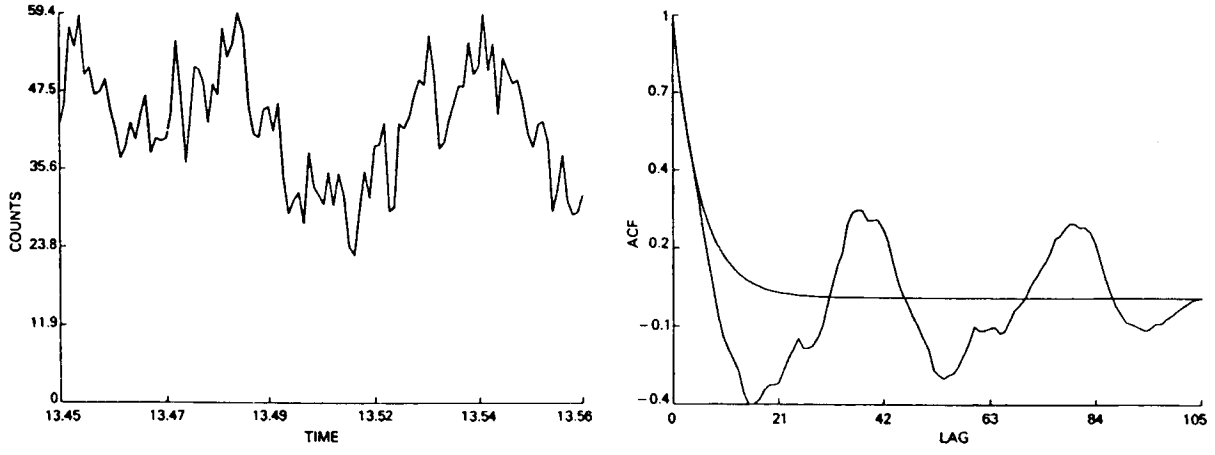

Figure 1a (left panel). Light curve representing an autoregressive series with a 17.5 s timescale fluctuation above a mean background of 42 counts. The series is generated using the algorithm described in the text. Time axis is in units of hours.

Figure 1b (right panel). Autocorrelation function of the above light curve (normalized to unity at zero lag). The smooth curve represents a fitted exponential with 20 s $1/e$ width. Time-lag axis is in units of 3.8 s accumulation bins.

2. OBSERVATIONS AND ANALYSIS

Flare 1 - GOES class M3 at UT 13:25 on 21 May 1984

This event was studied by Kaufmann *et al.* (1984), who demonstrated that hard X-ray structures and intensity fluctuations at 90 Ghz were well-correlated during the burst phase. Figure 2a indicates that hard X-ray fluctuations persisted with much weaker intensity for several minutes beyond the initial hard X-ray burst and were evidently correlated with soft X-ray features in the BCS Fe XXV (1.85 Å) and Ca XIX (3.18 Å) channels; with typical delays of less than 10 s.

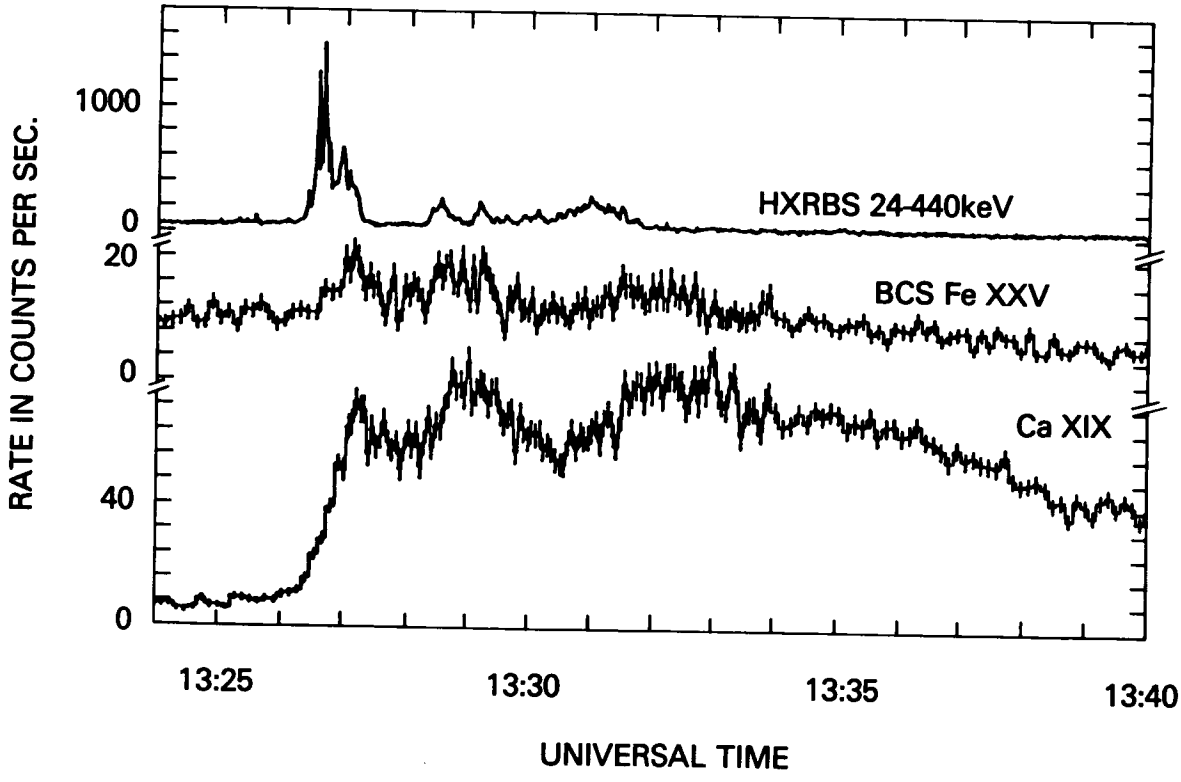

Figure 2a. HXRBS (1 s resolution) and BCS (3.8 s resolution) light curves are compared for flare 1. After the initial hard X-ray burst, there appear to be quasi-periodic fluctuations in the three light curves. Error bars denote σ variations

Figures 3a-c illustrate the HXRBS and BCS light curves in the period following the initial hard X-ray burst. The poisson error bars indicate that rapid 2-3 σ level fluctuations are present within the longer-term variation. Figures 4a-c show the corresponding autocorrelation functions for the above light curves. The fluctuation timescales implied by the $1/e$ widths are 14.1, 17.7, and 14.6 s for the HXRBS, Fe XXV, and Ca XIX light curves, respectively, with associated errors of $\pm$ 4 s. Hence, to within our measurement errors, the soft and hard X-ray emissions following the initial burst in flare 1 fluctuate with similar timescales of 15 - 20 s. Equivalently, the X-ray rise and decay times are typically faster than 10 s.

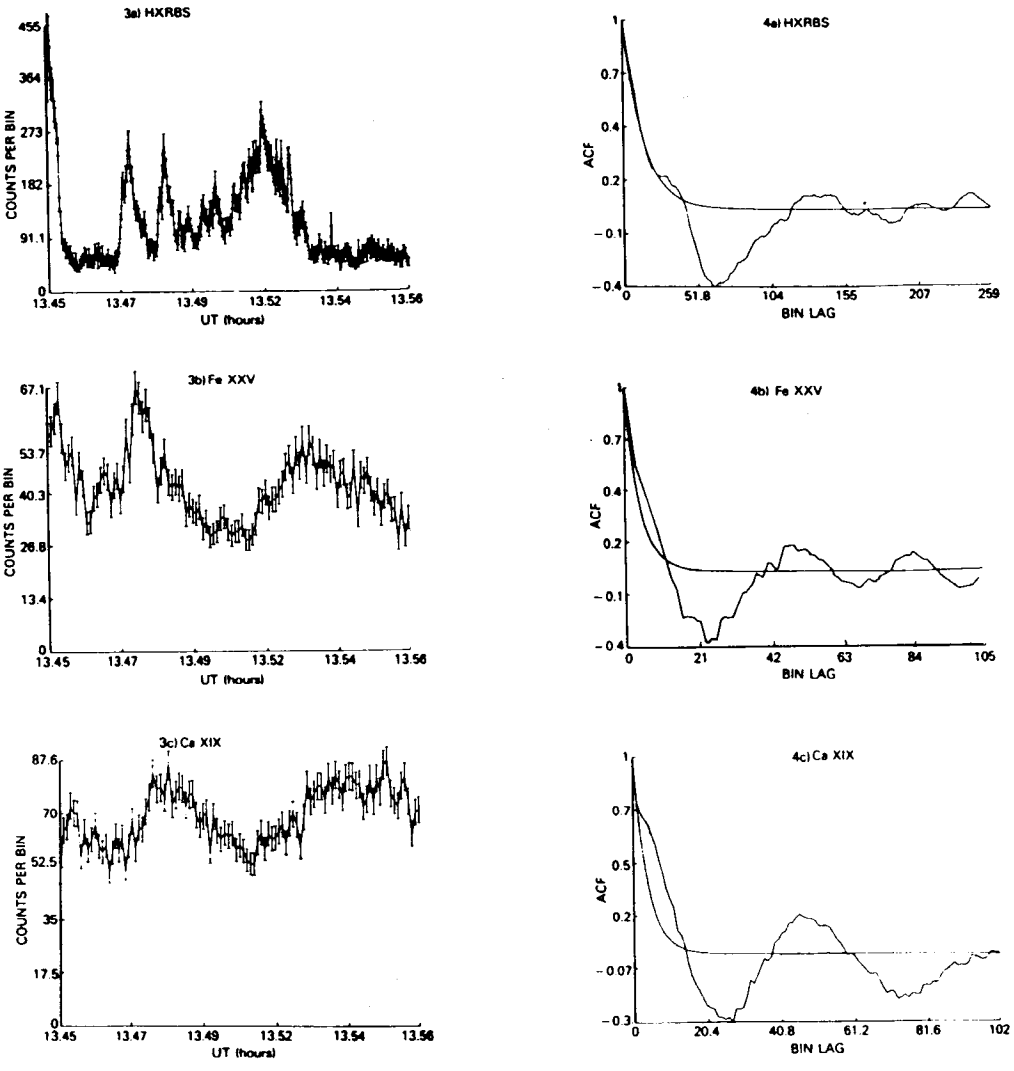

Figure 3a-c (left panel). Post impulsive phase light curves for flare 1 commencing at UT 13:27 are shown with σ poisson error bars. Intensity is in units of counts per bin resolution.

Figure 4a-c (right panel). Corresponding autocorrelation functions for the above curves with fitted exponentials.

Flare 2 - GOES class C3/M2 at UT 12:48 on 8 August 1980

Figure 2b illustrates the double event nature of this strong flare, with the second component (M2) exhibiting rapid fluctuations in the BCS Ca XIX light curve. As in flare 1, these soft X-ray features corresponded to specific hard X-ray spikes. From an autocorrelation function analysis of the second event, we inferred a characteristic spike width of 15 $\pm$ 5 s in both soft and hard X-rays. Note that this timescale is similar to the mean value obtained in flare 1.

The dynamics of flare 2 was studied by Strong *et al.* (1984), who found that the evolution of the second event was influenced significantly by the thermodynamic initial conditions created

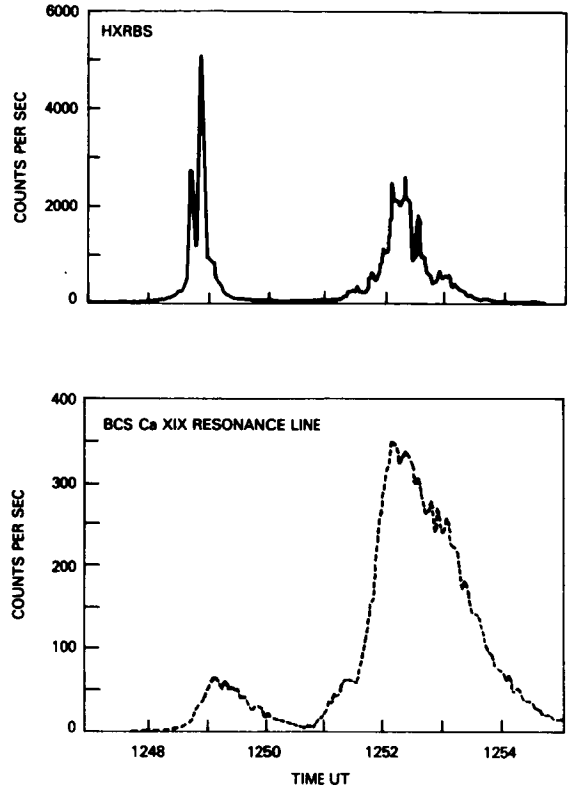

Figure 2b. HXRBS (top panel) and BCS Ca XIX (lower panel) light curves for the double-event flare 2. Note the prominence of fluctuations in hard and soft X-rays at approximately UT 12:53.

by the first event. In particular, prior to the first event, coronal plasma was relatively cool ($T_e \approx 3 \times 10^6$ K) and tenuous ($N_e \approx 4 \times 10^9 cm^{-3}$). However, at the onset of the second event, the temperature and density had both increased ($T_e \approx 5 \times 10^6$K, $N_e \approx 3 \times 10^{11} cm^{-3}$) due to previously heated chromospheric material being evaporated into the corona. Accordingly, Strong *et al.* (1984) suggested that a large fraction of the energy emitted subsequent to the first event would be absorbed high in the hot dense corona, with only a small proportion reaching the denser transition region and chromosphere. In view of this circumstance, we speculate that the rapid soft X-ray fluctuations that characterize the second event are a consequence of local heating by energy deposition in the upper flaring corona. This model will be examined further in section 3.

Flare 3- GOES class M3 at UT 01:25 on 20 May 1984

This flare exhibited fast fluctuations in the high-temperature FCS channels during the rise and decay phase of the soft component. The FCS Fe XXV channel light curve is shown in figure 2c. We used a 1 min running mean of the data to approximate the soft X-ray background and then subtracted it to produce the residuals shown in the upper curve. Comparison with

the HXRBS light curve reveals a close correspondence between features, with FCS fluctuations being most prominent in the post-impulsive phase. From an autocorrelation analysis of the Fe XXV residuals, we derived a fluctuation timescale of 12 $\pm$ 5 s, which is comparable with timescales determined for the previous two flares.

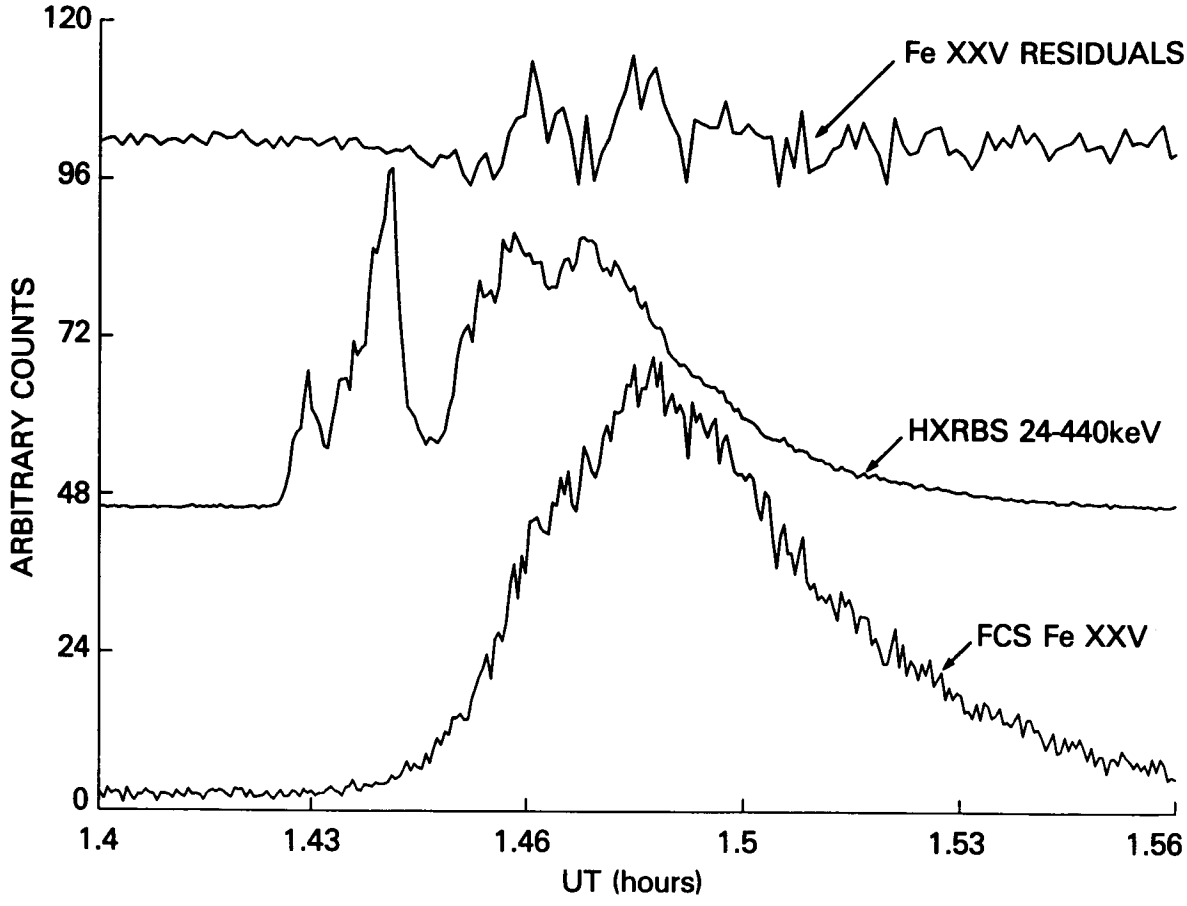

Figure 2c. FCS Fe XXV light curve (lower) for flare 3 is plotted at 2 s resolution. The middle curve shows the hard X-ray counterpart at equivalent resolution. The upper curve displays the Fe XXV residuals (magnified x 10) obtained after subtraction of a 1 min running mean of the FCS light curve. There is good qualitative correspondence between variations in the residuals and hard X-ray features. Note that the soft X-ray fluctuations became prominent after the initial hard X-ray burst.

To a first approximation, we can assess the statistical significance of these fluctuations by computing the deviation of the FCS residuals from the mean soft X-ray background. For example, figure 5 illustrates the Fe XXV residuals during the the first 1 min of the gradual rise phase plotted with constant σ lines (σ calculated from the square root of the smoothed soft

X-ray background). There are two features (A and B) that rise 2 to 3 σ above the background.

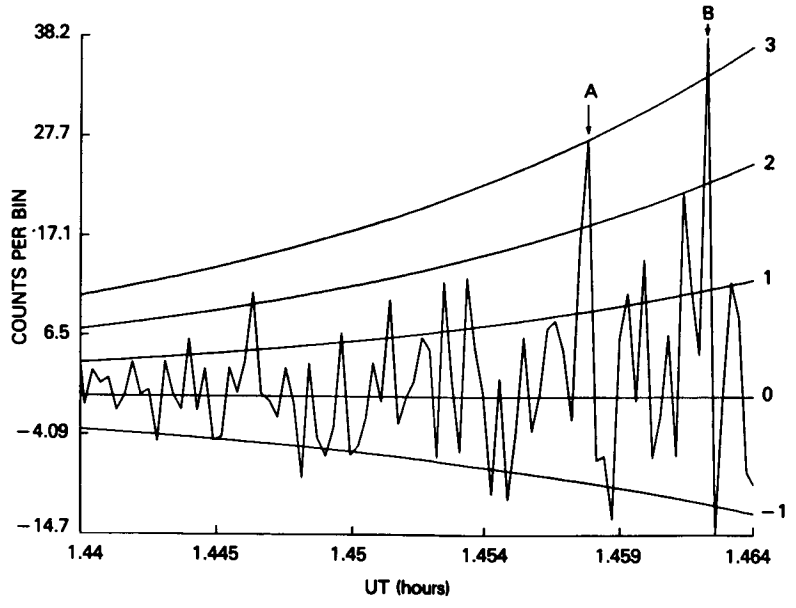

Figure 5. FCS Fe XXV residuals during the first 1 min of flare 3, plotted at 0.256 s resolution. The curves of constant σ are computed by assuming poisson counting statistics. Two features (A and B) lie approximately 3σ above the background.

Further analysis of this flare revealed that the prominence of fast intensity fluctuations decreased in the cooler-temperature sensitive FCS channels. For example, in figure 6 we compare the Fe XXV ($T_e \approx 2 \times 10^7$ K) channel light curve with the less temperature sensitive S XV (5×10^6 K) and Mg XI (3×10^6 K) channel light curves obtained simultaneously. The lack of stong fluctuations in the cooler-ion channels is further indication that these fluctuations are temperature-related phenomena. In particular, Peres *et al.* (1985) have indicated that the Fe XXV light curve represents the shape of the heating function, with the Fe XXV emissivity function being very steep at typical flare temperatures of 15 - 20 x 10^6 K. Accordingly, sudden temperature changes produced by heating would be strongly reflected as rapid changes in Fe XXV intensity. By contrast, the emissivity functions for the lower temperature sensitive ions such as Mg XI are broader and, thus, less responsive to sudden temperature changes.

3. DISCUSSION

The gradual soft X-ray phase of a flare is the response of the corona to the initial energy release – presumably characterized by the hard X-ray burst – and the thermalization of the non-thermal energy components of the flare (Strong *et al.* 1984). During the flare impulsive stage, energy is deposited deep down in the transition region and chromosphere. Whether this energy

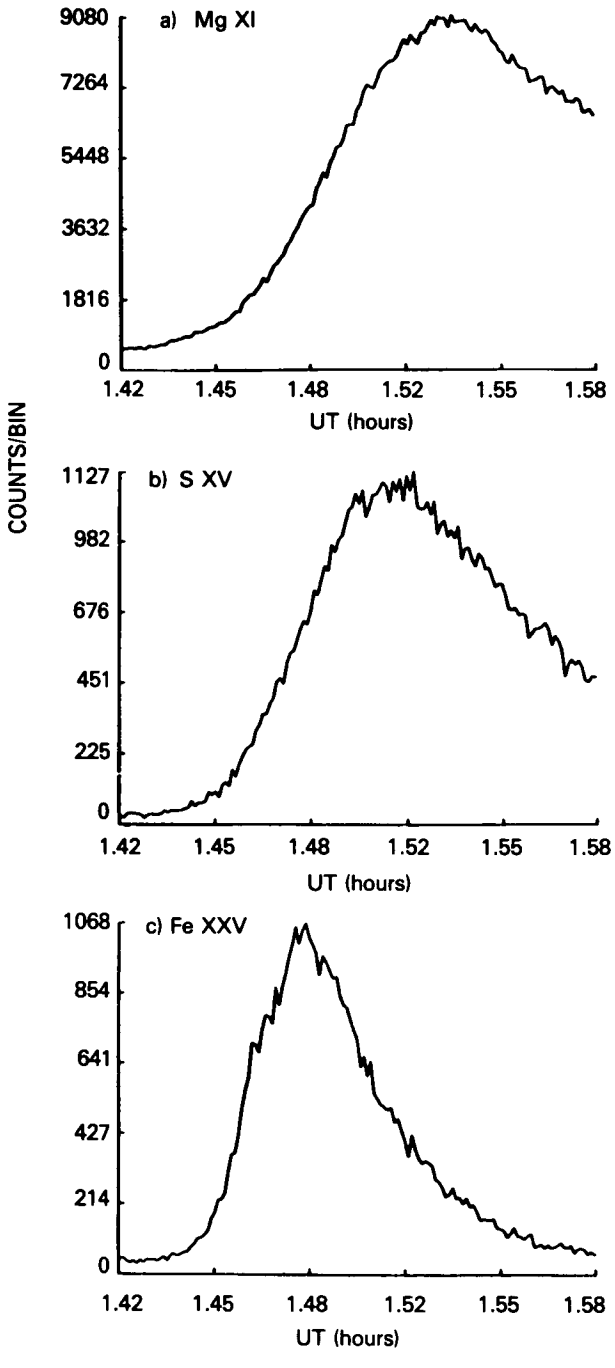

Figure 6a-c. FCS light curves of Mg XI, S XV, and Fe XXV, respectively, for flare 3 flare plotted at 4 s resolution. Note the decreasing prominence of fast spikes in the cooler-temperature sensitive channels.

is transported by a particle beam or by a thermal conduction front, chromospheric evaporation should result. This phenomenon is commonly observed as a high-velocity ($V \approx 400 \mathrm{kms}^{-1}$) stream of hot ($T_e > 10^6$ K) coronal plasma (Antonucci *et al.* 1982). The timescale to fill typical coronal loops of about 10^9 cm length is of the order of 30 s, which is comparable with the observed delay time between the hard and soft X-ray maxima.

The observations reported in this paper provide evidence for fast soft X-ray flare fluctuations with timescales that are shorter than expected for simple hydrodynamic processes. For example, an upward velocity in excess of 1000 km s^{-1} would be required to evaporate hot, dense chromospheric material sufficiently fast to produce a 10 s soft X-ray enhancement. Such a large blueshift was not observed in, for example, the BCS Ca XIX resonance line wing. Consequently, the observed intensity brightenings in soft X-rays are more probably due to local temperature enhancements that occur in the upper layers of the flaring coronal loop. This is consistent with our observation that the rapid soft X-ray fluctuations often corresponded with hard X-ray emissions.

The amplitudes of the soft X-ray fluctuations were typically less than 20% in the three flares studied. Based on the theoretical emissivity functions for Ca XIX and Fe XXV, such intensity changes would require a temperature increase of about 5 x 10^6 K. A possible driver for this increase could be magnetic reconnection occuring after the initial hard X-ray burst. Following each local heating episode, the hot plasma is likely to cool conductively within a timescale given by the expression:

$$\tau_c \approx 2 \times 10^{-10} N_e L^2 T_e^{-5/2},$$

where L denotes the conductive lengthscale (Svestka 1976). Setting $T_e \approx 2 \times 10^7$ K for the enhanced temperature of the soft X-ray emitting plasma (Strong *et al.* 1984), assuming $N_e \approx 10^{11} \mathrm{cm}^{-3}$ as characteristic of the peak coronal electron density (Veck *et al.* 1984), and adopting the 10 s soft X-ray decay time as representative of τ_c, we derive $L \approx 10^8$ cm. Note that this value is an order of magnitude less than typical loop lengths, indicating that the locally injected heat energy is conducted quite rapidly into the surrounding cooler medium. This is in contrast with the energy associated with the initial hard X-ray burst, which is dissipated over much longer length scales ($L \approx 10^9$ cm).

4. CONCLUSIONS

We have presented evidence for fast soft X-ray fluctuations during the onset of the gradual component in three solar flares. These variations occurred in conjunction with similar features in hard X-rays, although they were not necessarily correlated in intensity. The timescales of these fluctuations were shorter than the typical hydrodynamic timescales expected for solar flares.

It is generally accepted that the initial hard X-ray burst in a solar flare is responsible for heating dense chromospheric material which subsequently evaporates into the corona. It is likely that in the ensuing soft X-ray gradual phase, secondary heating may occur (e.g., by magnetic reconnection). Since the coronal density is already enhanced by evaporation ($N_e > 10^{11} \mathrm{cm}^{-3}$), this energy is absorbed *in situ* rather than being transported to lower transition region layers. We have speculated that such secondary heating may be responsible for the observed soft X-ray intensity spikes. A more detailed study of this mechanism would demand theoretical calculations that are beyond the scope of this exploratory investigation. However, past numerical simulations

of rapid heating of coronal loop plasma predict that, among the many non-equilibrium effects to arise, burst-like enhancements in soft X-ray flux are indeed likely to be a very common phenomenon (Shapiro and Moore 1977).

Acknowledgements

This work was performed at the Goddard Space Flight Center and supported by NASA contract NASS-28713 and the Lockheed Independent Research Programme. We thank Allyn F. Tennant for helpful discussions on autocorrelation techniques.

REFERENCES

Acton, L. W., *et al.* 1980, *Solar Phys.*, **65**, 53.

Antonucci, E., *et al.* 1982, *Solar Phys.*, **78**, 107.

Jenkins, G.M., and Watts, D.C. 1968, in *Spectral Analysis and its Applications*, ed. (San Francisco: Holden-Day).

Kaufmann, P., Correia, E., Costa, J.E.R, Zodi Vaz, A.M., and Dennis, B.R. 1985, *Nature*, **313**, 380.

Peres, G., Serio, S., and Pallavicini, R. 1985, submitted to *Astrophys. J.*

Shapiro, P.R., and Moore, R.T. 1977, *Ap. J.*, **217**, 621.

Strong, K.T., *et al.* 1984, *Solar Phy.*, **91**, 325.

Svestka, Z. 1976, in *Solar Flares*, ed. (Reidel: Dordrecht).

Veck, N.J., Strong, K.T., Jordan, C., Simnett, G.M., Cargill, P.J., and Priest, E.R. 1984, *M.N.R.A.S.*, **210**, 443.